

STRUCTURE AND PHOTOLUMINESCENCE PROPERTIES OF SnO₂ NANOWIRES SYNTHESIZED FROM SnO POWDER

© 2009 E. P. Domashevskaya¹, N. M. A. Hadia^{1,2}, S. V. Ryabtsev¹, P. V. Seredin¹

¹ Voronezh State University, Universitetskaya pl. 1, 394006, Voronezh, Russia

² Department of physics, Faculty of Science, Sohag University, 82524-Sohag, Egypt

Received to editor 22.11.2008

Abstract. One-dimensional (1D) SnO₂ nanowires were synthesized from SnO powder by heat treatment of SnO powder under Ar gas flow at atmospheric pressure, with the next annealing on the air at 1000° C. The morphology and microstructure of the single crystalline SnO₂ nanowires are characterized by means of the X-ray diffraction (XRD) and scanning electron microscopy (SEM). The band gaps of the products are ~ (3.42—3.78 eV) determined from UV/visible absorption spectral results. The SnO₂ nanowires show stable photoluminescence (PL) with one emission peak centred at around ~ 2.00 eV.

Keywords: Nanowires, SnO, SnO₂, structure, photoluminescence and optical.

INTRODUCTION

During recent decades, nanostructured materials have received considerable attention from the scientific and engineering communities [1]. These structures exhibit distinct properties from those of bulk materials due to their small size and large surface-to-volume ratios, and accordingly, nanostructured materials have emerged as promising candidates for realizing nanoscale electronic, optical, and mechanical devices with enhanced performance. Among them, one-dimensional (1D) nanomaterials, such as nanowires, nanotubes and nanobelts can function as both nanoscale device elements and interconnects while keeping unique properties due to size confinement in the radial direction [2]. Therefore, 1D nanostructures, in particular, semiconductor 1D nanostructures have been successfully synthesized by various methods such as thermal evaporation [3], chemical vapor deposition [4], laser ablation [5], template [6], and sol-gel [7] techniques. Their optical, electronic, and magnetic properties as well as their potential use in various applications have also been extensively investigated.

Nanocrystals emerged earlier than 1D nanostructures, partly due to the fact that they are readily generated via various experimental methods. These manufacturing methods include: melt crystallization, chemical vapor deposition (CVD), laser, self-propagating high-temperature synthesis (SHS), hydrothermal processes and others [8]. Nanocrystals have wide

application in the electronic, optical, mechanical, magnetic, and sensing materials fields [9].

SnO₂, an *n*-type wide band gap ($E_g = 3.6$ eV, at 300 K) semiconductor with appreciable degree of ionicity, is attractive for potential applications in gas sensors [10], catalyst supports [11], and transparent conducting electrodes [12]. Recently, a series of SnO₂ nanobelts, nanowires, and nanocrystals have been synthesized and investigated [13]. However, systematic comparisons and investigations of the relationship between microstructures and properties of the above different morphologies and optical properties of 1D SnO₂ nanostructures are still unclear [14].

Optical measurements such as optical band gap and photoluminescence (PL) are very useful for the determination of the structure, defects, and impurities in these nanostructures, and there have been several reports on the optical band gap and luminescence of 1D SnO₂ nanostructures at room temperature [15] showing emission in the range 2.00—3.10 eV. The luminescence is generally believed to stem from defects such as tin interstitials, dangling bonds, or oxygen vacancies. However, direct proof that such defects are incorporated in the luminescence centre has not yet been given.

In this paper, the morphological, structural, optical properties and photoluminescence (PL) of quasi-one-dimensional (1D) SnO₂ nanowires were synthesized from SnO powder by heat treatment of SnO powder under Ar gas flow at atmospheric pressure, with the

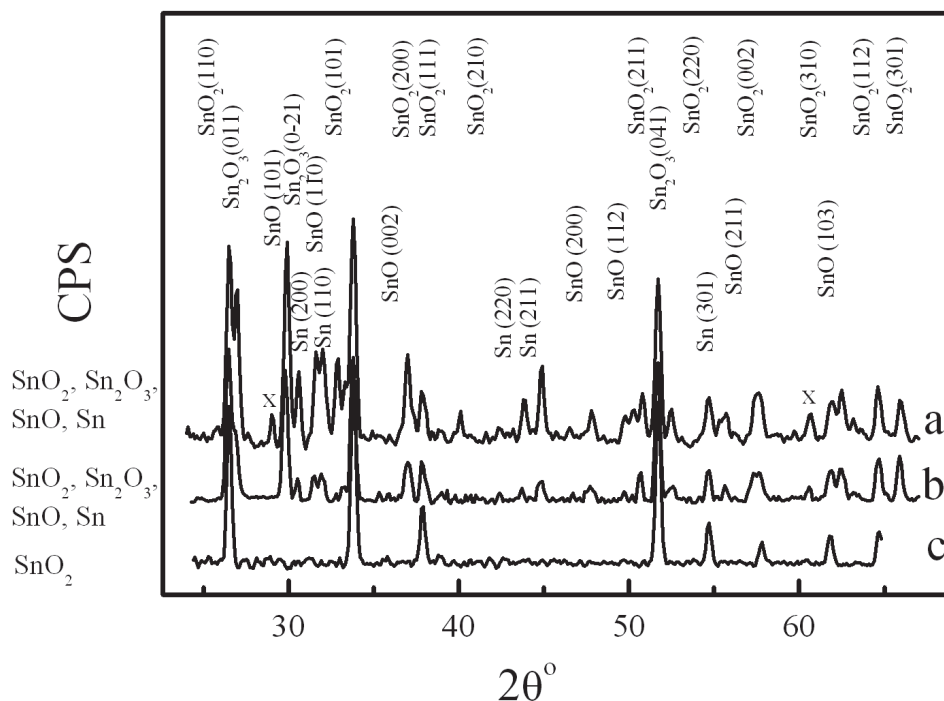


Fig. 1. X-ray diffraction patterns of the (sample *a* with the “gray color”), (sample *b* with the “white color”) and (sample *c* is the *b*, annealed at 1000°C).

next annealing on the air at 1000°C are presented as a function of the preparation samples and the temperature of annealing. The experimental details have already been described by [16].

EXPERIMENTAL TECHNIQUE

In our materials synthesis, a 100 cm long horizontal quartz tube with an inner diameter of 50 mm open on one side was mounted inside a high-temperature quartz tube furnace. 99.99% pure SnO powders were placed in an alumina boat positioned at the centre of the quartz tube. The temperature in the furnace was rapidly ramped up to 1050–1100°C kept for 90 min. During the process, a constant flow of Ar (99.99%) at a rate of 50 sccm was maintained. The morphology and crystal structure of the synthesized nanostructures were characterized by x-ray diffraction (XRD) using a DRON 4 utilizing Cu K α radiation, scanning electron microscopy (SEM) employing a JSM-6380LV. UV/visible absorption measurements were carried out on the SnO₂ nanowires using a spectrophotometer (UV-210A, Shimadzu) in a range between 90 and 900 nm. The Photoluminescence (PL) spectra were using for excitation a 337 nm ILGI 503 N2 laser.

RESULTS AND DISCUSSION

In beginning must be observed that, Samples prepared in gas-transport synthesis, had various color. In

the sample (a) of “gray color” are present the larger drops (droplets) of metal tin on the ends of crystals. These drops will lend gray color to sample. Diffractogram acknowledge it. In the sample (b) of the “white color” of such metal drops on the ends of crystals few or they item much less size. “Gray” and “white” samples were received in the various conditions of synthesis, but the sample (c) is the same the sample (b) of the “white color” but heat treatment at the temperature 1000°C.

The structure and phase of the three samples as revealed by XRD are depicted in figure 1. Both samples (a and b) possess the same structure that can be indexed to a pure rutile phases SnO₂, Sn₂O₃, SnO and Sn but sample (c) possess the structure that can be indexed to a pure rutile phase SnO₂ with lattice constants of $a = 4.738 \text{ \AA}$ and $c = 3.189 \text{ \AA}$. Figure 2 show typical scanning electron microscopy (SEM) images of the synthesized product. It indicated that the SnO₂ nanowires are long and straight, and the surface is pure enough. The cross-section size crystallite $\sim 100 \text{ nm}$, the attitude cross-section to the longitudinal size $\sim 1000 \text{ Micro}$ drops of tin on the ends crystallite testify to the mechanism of their growth of pairs-metals-crystals.

It is well known that SnO₂ is a degenerate semiconductor with band gap energy (E_g) in the range of 3.4–4.6 eV [17]. This scatter in band gap energy (E_g) of SnO₂ may be due to varied extent of non-stoichi-

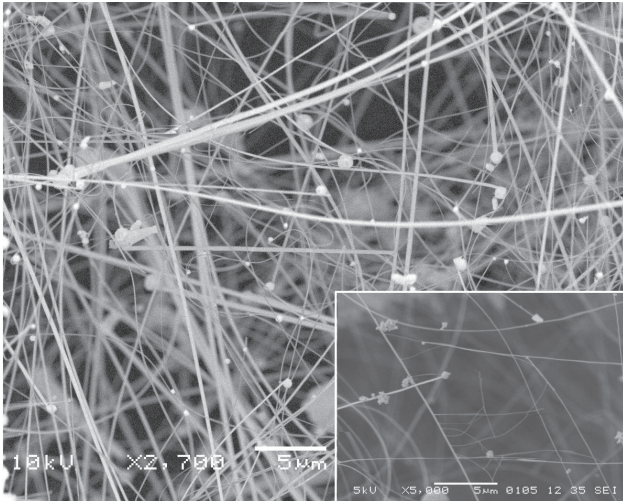


Fig. 2. Scanning electron microscopy (SEM) image of the synthesized SnO₂ nanowires.

ometry of the deposited layers. The dependency of the band gap energy on the carrier concentration has been explicitly given in the literature [18]. It has been

apprehended that band gap energy increases linearly with the increase in carrier concentration to the power 2/3. High-energy shift of an absorption edge is generally expected for nanocrystalline materials. In order to confirm this, absorption spectra were acquired from the SnO₂ nanowires, and the results are depicted in figure 3 (a) and 3 (b). The optical transition of SnO₂ crystals is known to be a direct type [18]. In this case, the absorption coefficient α is expressed as $\alpha(h\nu) \propto (h\nu - E_g)^{1/2}/h\nu$ [19]. Plots of $(\alpha(h\nu))^2$ versus $h\nu$ can be derived from the data in figure 3. The intercept of the tangent to the plot gives a good approximation of the band gap energy of the direct band gap materials. This is ~3.42 eV for the sample (a) and ~3.78 eV for the samples (b) and (c), as shown in the inset of figure 3(b); both of which are larger than the value of 3.62 eV for bulk SnO₂ due to the quantum size effect [20]. In addition, the larger band gap of the samples (b) and (c) than that of the sample (a) also agrees well with their observed from X-ray examinations.

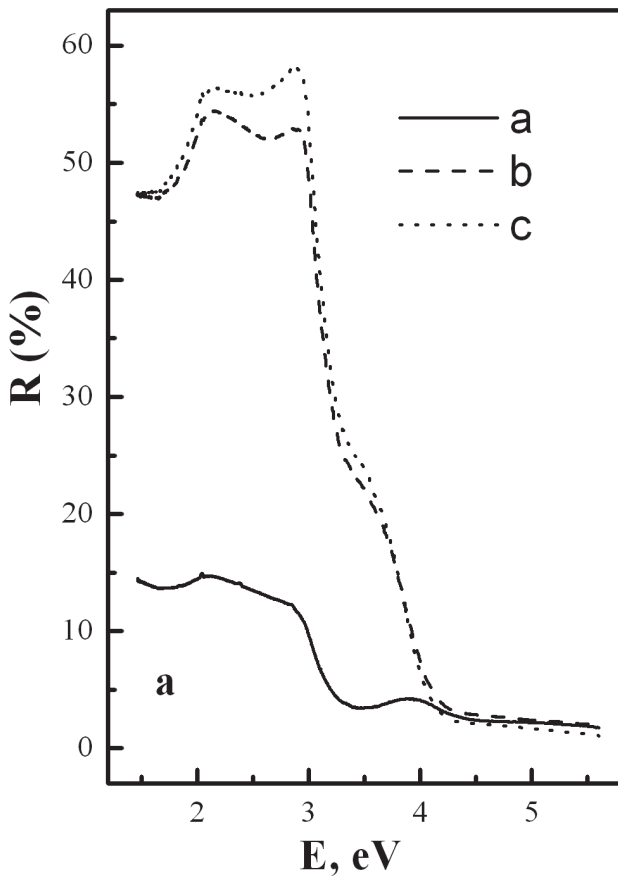


Fig. 3a. Spectral variations of Reflectance (R) for SnO₂ nanowires for the (sample a with the “gray color”), (sample b with the “white color”) and (sample c annealed at 1000° C).

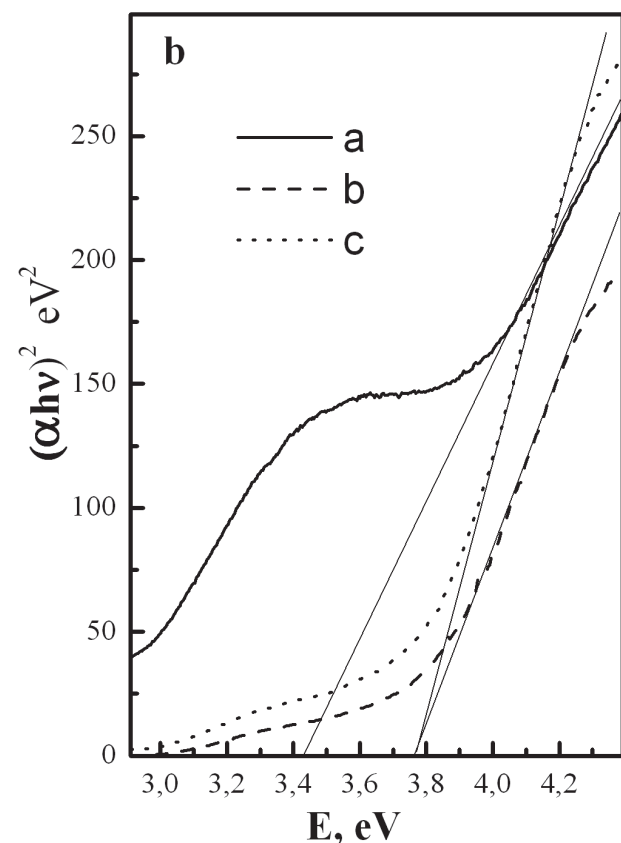


Fig. 3b. $(\alpha(h\nu))^2$ versus photon energy curve for SnO₂ nanowires for the (sample a with the “gray color”), (sample b with the “white color”) and (sample c annealed at 1000° C).

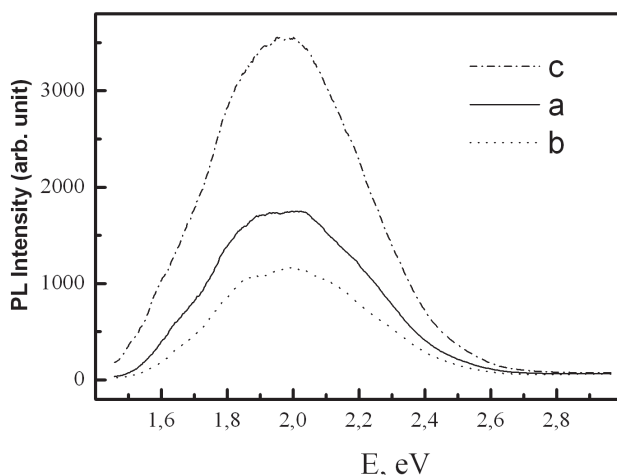


Fig. 4. Photoluminescence (PL) spectra of the SnO₂ nanowires for the (sample a with the “gray color”), (sample b with the “white color”) and (sample c annealed at 1000° C).

Figure. 4 shows the variation of photoluminescence emission intensity of tin oxide nanowires as a function of samples preparations and the temperature. In all the cases, a strong green emission band was observed around ~ 591 nm with an energy gap of 2.00 eV. This emission is attributed to the crystal defects or the electron transition mediated by defect levels such as oxygen vacancies, tin interstitials and so on in the band gap during the growth. Generally, oxygen vacancies are known to be the most common defects and usually act as radiative centres in luminescence processes. The oxygen vacancies present in three different charge states V_o^0 , V_o^+ and V_o^{++} in the semiconductor oxides [21]. As V_o^0 is a very shallow donor, the most oxygen vacancies will be in their paramagnetic V_o^+ state under flat-band conditions. Hence, the origin of the green emission band in the PL spectrum of SnO₂ nanowires is assigned to the recombination of electrons in the singly occupied oxygen vacancies with photoexcited holes in the valance band [22]. A similar observation was made earlier in the PL spectrum of SnO₂ nanostructural material by Hu et al. [23]. As the calcinations temperature increases to 1000° C, the particle size of tin oxide in nanowires becomes larger and hence a increase in the PL intensity 2.00 in the luminescence spectra can occur resulting from the reductions of both the surface area and concentration of oxygen vacancies.

All this emission peaks can be attributed to the trap emission. It is usually thought that point defects such as oxygen vacancies are in existence [24, 25]. It is suggested that the emission peaks to electron transition

is mediated by defect levels in the band gap, such as oxygen vacancies. In the present SnO₂ nanostructure, the intrinsic defects, such as oxygen vacancies, which act as luminescent centers, can form defect levels located highly in the gap, trapping electrons from the valence band to make a contribution to the luminescence. Generally, oxygen vacancies are known to be the most common defects and usually act as radiative centers in luminescence processes.

SUMMARY

In summary, One-dimensional (1D) SnO₂ nanowires were synthesized from SnO powder by heat treatment of SnO powder under Ar gas flow at atmospheric pressure. The temperature in the furnace was rapidly ramped up to 1050—1100° C kept for 90 min. The optical direct band gap lies in range between 3.42 and 3.78 eV. The microstructures of the SnO₂ nanowires were characterized. The morphology of the products depends on the methods preparations and reaction temperature. The room temperature PL spectra of the SnO₂ nanowires showed a strong green band emission at ~ 591 nm with a band gap of ~ 2.10 eV, which is associated with oxygen vacancies or surface defect states. It is therefore highly promising for use in optoelectronic devices.

REFERENCES

1. Dai H. J., Wong E. W., Lieber C. M. et. al. // Science. 1996. V. 272. P. 523—526.
2. Huang M. H., Mao S., Feick H., Yan H. Q., Wu Y., Kind H. et. al. // Science. 2002. V. 292. P. 183107—1—3.
3. Li Y., Qian L. H., Li W. F., Yang C. N., Ma X. L. et. al. // Appl. Phys. Lett. 2005. V. 86. P. 1897—1899.
4. Li Y., Ma X. L. et. al. // Physica Status Solidi A. 2005. V. 202. P. 2079—2084.
5. Morales A. M., Lieber C. M. et. al. // Science. 1998. V. 279. P. 208—211.
6. Wang W., Li N., Li X. T., Geng W.C., Qiu S. L. et. al. // Mat. Res. Bull. 2006. V. 41. P. 1417—1427.
7. Lei Y., Zhang L. D., Meng G. W., Li G. H., Zhang X. Y., Liang C. H., Chen W., Wang S. X. et. al. // Appl. Phys. Lett. 2001. V. 78. P. 1125—1127.
8. Wu M. M., Lin G., Chen D. H., Wang G. G., He D., Feng S.H., Xu R. R. et. al. // Chemistry of Materials 2002. V. 14. P. 1974—1980.
9. Liu Z. T., Lee C., Narayanan V., Pei G., Kan E. C. et. al. // IEEE Transaction on electron devices 2002. V. 49. P. 1606—1611.
10. Comini E., Faglia G., Sberveglieri G., Z. W. Pan, Wang Z. L. et. al. // Appl. Phys. Lett. 2002 V. 81. P. 1869—1871.
11. Dazhi W., Shulin W., Jun C., Suyuan Z., Fangqing L. et. al. // Phys. Rev. B. 1994. V. 49. P. 282—287.

12. He Y. S., Campbell J. C., Murphy R. C., Arendt M. F., Swinnea J. S. et. al. // J. Mater. Res. 1993. V. 8. P. 3131—3134.
13. Chen Y. J., Li Q. H., Liang Y. X., Wang T. H., Zhao Q., Yu D. P. et. al. // Appl. Phys. Lett. 2004. V. 85. P. 5682—5684.
14. Hu J. Q., Ma X. L., Shang N. G., Xie Z. Y., Wong N. B., Lee C. S., Lee S. T. et. al. // J. Phys. Chem. B. 2002. V. 106. P. 3823—3826.
15. Faglia G., Baratto C., Sberveglieri G., Zha M., Zappettini A., et. al. // Appl. Phys. Lett. 2005. V. 86. P. 11923—11925.
16. C. Zhao Xu, X., Liu S., Wang G. et. al. // Solid State Commun. 2003. V. 125. P. 301—304.
17. Rakshani A. E., Makdisi Y., Ramazanyan H. A. et. al. // J. Appl. Phys. 1998. V. 83. P. 1049—1055.
18. Frohlich D., Kenklies R. et. al. // Phys. Rev. Lett. 1978. V. 41. P. 1750—1751.
19. Mills G., Li Z. G., Meisel D. et. al. // J. Phys., Chem. 1988. V. 92. P. 822—830.
20. Brus L., Chem J. et. al. // Phys. 1983. V. 79. P. 5566—5571.
21. Zhzng W. F., Zhang M. S., Yin Z., Chen Q. et. al. // Appl. Phys. B. 2000. V. 70. P. 261—265.
22. Vanheusden K., Warren W. L., Seager C. H., Tallant D. R., Voigt J. A., Gnade B. E. et. al. // J. Appl. Phys. 1996. V. 79. P. 7983—7990.
23. Hu J. Q., Y. Bando, Golberg D. et. al. // Chem. Phys. Lett. 2003. V. 372. P. 758—762.
24. Chiodini N., Paleari A., DiMartino D., Spinolo G. et. al. // Appl. Phys. Lett. 2002. V. 81. P. 1702—1704.
25. Gu F., Wang S. F., Song C. F., Lv M. K., Qi Y. X., Zhou G. J., D. Xu, Yuan D. R. et. al. // Chem. Phys. Lett. 2003. V. 372. P. 451—454.

Домашевская Эвелина Павловна — д.ф.м.н., профессор, Воронежский государственный университет; e-mail: ftt@phys.vsu.ru

Хадиа Н.М.А. — аспирант, Воронежский государственный университет; e-mail: nomery_abass@yahoo.com

Рябцев Станислав Викторович — к.х.н., Воронежский государственный университет; e-mail: ftt@phys.vsu.ru

Середин Павел Владимирович — к.ф.-м.н., Воронежский государственный университет; e-mail: paul@phys.vsu.ru

Domashevskaya Evelina. P. — the doctor of physical and mathematical sciences, the professor, Voronezh State University; e-mail: ftt@phys.vsu.ru

Hadia N. M. A. — post graduate student of Department of physics, Faculty of Science, Sohag University; e-mail: nomery_abass@yahoo.com

Ryabtsev Stanislav V. — candidate of chemical sciences, Voronezh State University; e-mail: ftt@phys.vsu.ru

Seredin Pavel V. — candidate of physical and mathematical sciences, Voronezh State University; e-mail: ftt@phys.vsu.ru